Life Sciences 222 (2019) 1–12

Contents lists available at ScienceDirect

Life Sciences

journal homepage: www.elsevier.com/locate/lifescie

Cholinergic drugs ameliorate endothelial dysfunction by decreasing O-GlcNAcylation via M3 AChR-AMPK-ER stress signaling

Yan-Ling Cui, Run-Qing Xue, Xi He, Ming Zhao, Xiao-Jiang Yu, Long-Zhu Liu, Qing Wu, Si Yang, Dong-Ling Li*, Wei-Jin Zang*

Department of Pharmacology, School of Basic Medical Sciences, Xi'an Jiaotong University Health Science Center, Xi'an, Shaanxi 710061, PR China

ARTICLE INFO

Keywords:
Obesity
O-GlcNAc
ER stress
Endothelial cell apoptosis
Cholinergic drugs
M3 AChR-AMPK

ABSTRACT

Aims: Obesity is associated with increased cardiovascular morbidity and mortality. It is accompanied by augmented O-linked β-*N*-acetylglucosamine (O-GlcNAc) modification of proteins via increasing hexosamine biosynthetic pathway (HBP) flux. However, the changes and regulation of the O-GlcNAc levels induced by obesity are unclear.

Main methods: High fat diet (HFD) model was induced obesity in mice with or without the cholinergic drug pyridostigmine (PYR, 3 mg/kg/d) for 22 weeks and *in vitro* human umbilical vein endothelial cells (HUVECs) was treated with high glucose (HG, 30 mM) with or without acetylcholine (ACh).

Key findings: PYR significantly reduced body weight, blood glucose, and O-GlcNAcylation levels and attenuated vascular endothelial cells detachment in HFD-fed mice. HG addition induced endoplasmic reticulum (ER) stress and increased O-GlcNAcylation levels and apoptosis in HUVECs in a time-dependent manner. Additionally, HG decreased levels of phosphorylated AMP-activated protein kinase (AMPK). Interestingly, ACh significantly blocked damage to HUVECs induced by HG. Furthermore, the effects of ACh on HG-induced ER stress, O-GlcNAcylation, and apoptosis were prevented by treating HUVECs with 4-diphenylacetoxy-*N*-methylpiperidine methiodide (4-DAMP, a selective M3 AChR antagonist) or compound C (Comp C, an AMPK inhibitor). Treatment with 5-aminoimidazole-4-carboxamide ribose (AICAR, an AMPK activator), 4-phenyl butyric acid (4-PBA, an ER stress inhibitor), and 6-diazo-5-oxonorleucine (DON, a GFAT antagonist) reproduced a similar effect with ACh.

Significance: Activation of cholinergic signaling ameliorated endothelium damage, reduced levels of ER stress, O-GlcNAcylation, and apoptosis in mice and HUVECs under obese conditions, which may function through M3 AChR-AMPK signaling.

1. Introduction

Obesity is associated with an increase in cardiovascular morbidity and mortality. In the vasculature, obesity induces endothelial dysfunction, structural remodeling of the vascular wall [1,2], and myocardial dysfunction and remodeling [3,4], resulting in the development of cardiovascular disease. Despite decades of research identifying the endothelium as the key in the origination and development of vascular damage, the potential mechanisms of endothelium damage have not been completely understood [5]. Recently, an increase in the levels of O-linked *N*-acetylglucosamine (O-GlcNAc) on nuclear and cytosolic proteins has been identified as a critical mediator of obesity-associated vascular damage and cardiovascular disease [6].

The hexosamine biosynthesis pathway (HBP) generates sugar nucleotide uridine diphospho-*N*-acetyl-glucosamine (UDP-GlcNAc), a substrate for protein O-linked β-*N*-acetylglucosamine modification (O-GlcNAcylation) [7]. O-GlcNAcylation is a post-translational modification that adds *N*-acetylglucosamine (GlcNAc) to serine or threonine residues of proteins. The reaction is catalyzed by O-linked *N*-acetylglucosamine transferase (OGT) and is reversed by the *N*-acetylglucosaminidase (OGA). Numerous nuclear, cytoplasmic, and mitochondrial proteins have been identified as O-GlcNAc modification targets. O-GlcNAcylation involves a variety of cellular activities, including the cellular nutrient sensing pathway [8] and cellular stress responses [9]. Normally, HBP metabolizes only 2–5% of glucose in cells. However, the rate of HBP can be regulated by substrate concentration, such as glucose and GlcNAc, and controlled by glucosamine-fructose-6-phosphate amidotransferase (GFAT), the rate limiting enzyme of HBP. Furthermore, augmented O-GlcNAcylation in the vasculature increases vasoconstriction and impairs

* Corresponding authors at: P.O. Box 77#, No.76 Yanta West Road, Xi'an Jiaotong University Health Science Center, Xi'an 710061, PR China.
E-mail addresses: lidl@xjtu.edu.cn (D.-L. Li), zwj@xjtu.edu.cn (W.-J. Zang).

https://doi.org/10.1016/j.lfs.2019.02.036
Received 12 December 2018; Received in revised form 15 February 2019; Accepted 17 February 2019
Available online 17 February 2019
0024-3205/

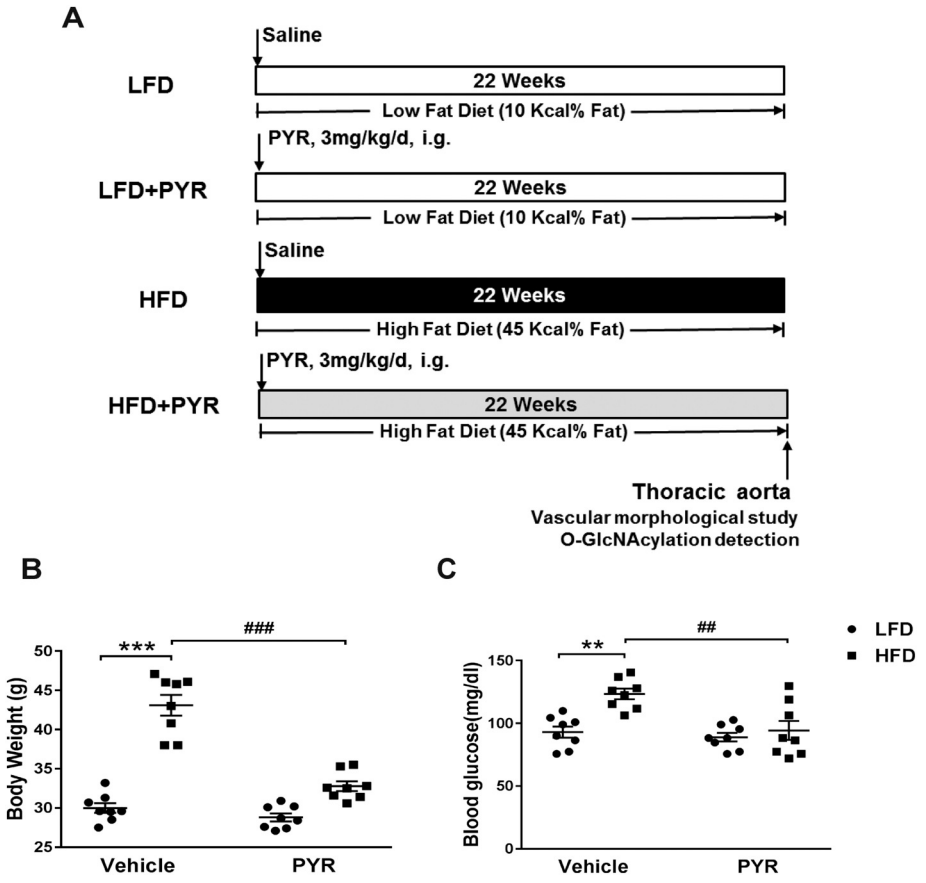

Fig. 1. Experimental protocol and the effects of PYR on body weight and blood glucose level in obese mice. A: Experimental protocol. B & C: Effects of HFD and PYR on body weight and blood glucose. Data represent mean ± SEM ($n = 8$). Two-way ANOVA showed that body weight was significantly affected by HFD ($P < 0.001$), PYR ($P < 0.001$), and their interaction ($P < 0.001$). For the blood glucose level the effect of HFD ($P < 0.01$), PYR ($P < 0.01$), and their interaction ($P < 0.05$) was observed. Significant between-group differences from post hoc Tukey test are given as follows: $^{**}P < 0.01$ vs. LFD: Vehicle, $^{***}P < 0.001$ vs. LFD: Vehicle; $^{\#\#}P < 0.01$ vs. HFD: Vehicle, $^{\#\#\#}P < 0.001$ vs. HFD: Vehicle. i.g.: intragastric administration.

endothelium-dependent vasodilatation [10]. Although the role of HBP in metabolism and various diseases is established, regulation of the HBP remains largely unknown. Recent evidence suggests that endoplasmic reticulum (ER) stress can lead to obesity-related complications. It is known that prolonged perturbation of ER stress contributes to endothelial and myocardial dysfunction, leading to various cardiovascular risks [11,12]. More recently, various studies showed that O-GlcNAcylation was associated with the ER stress response. For example, glucosamine treatment upregulated O-GlcNAc flux through HBP, and induced the expression of the ER stress marker GRP78 [13]. Similarly, ER stress inducers promoted O-GlcNAcylation [14–16]. However, the interaction and relationship between O-GlcNAcylation and the ER stress in obesity and hyperglycemia is unclear.

Accumulating evidence indicates that obesity is accompanied with an increase in sympathetic activity and a decrease in vagal activity [17–19]. Our previous data revealed that pyridostigmine (PYR) increased serum acetylcholine (ACh) levels, improved cardiac function in obese rats [20], and protected endothelial ultrastructure integrity in myocardial infarction rats [21]. Furthermore, studies from our laboratory showed that ACh exhibits protective effects against hypoxia/reoxygenation-induced human umbilical vein endothelial cell (HUVECs) apoptosis via activation of adenosine 5′-monophosphate-activated protein kinase (AMPK) [22]. However, the role of M3 AChR/AMPK in O-GlcNAcylation in HUVEC during obesity remains unknown. In the present study, we investigated the role of cholinergic drugs (PYR and ACh) in the protection of thoracic arterial endothelial damage from obesity-induced O-GlcNAcylation, explored how aberrant ER stress and O-GlcNAcylation were involved in hyperglycemia-induced endothelial injury, and determined how ACh functions as an AMPK activator to reduce ER stress, O-GlcNAcylation, and subsequent cell apoptosis.

2. Materials and methods

2.1. Reagents

Pyridostigmine (PYR) was purchased from Shanghai Zhongxi Sunve Pharmaceutical (Shanghai, China), whereas acetylcholine (ACh), D-glucose, glucosamine (GlcN), 5-aminoimidazole-4-carboxamide ribose (AICAR), 4-phenyl butyric acid (4-PBA), 6-diazo-5-oxonorleucine (DON), and 4-diphenylacetoxy-*N*-methylpiperidine methiodide (4-DAMP) were purchased from Sigma (Sigma-Aldrich, St Louis, MO, USA). Compound C (Comp C) was purchased from MedChem express (New Jersey, USA). These reagents were dissolved in an appropriate solvent according to the manufacturers' instructions, and then sterile-filtered and added into cultured cells at indicated concentrations. All other chemicals used in our experiments were of analytical reagent grade.

2.2. Animals

All experimental procedures in this study were in accordance with the Guide for the Care and Use of Laboratory Animals (National Institutes of Health Publication no. 85-23, revised 1996) and approved by the Ethics Committee of Xi'an Jiaotong University. 4-week-old C57BL/6J male mice were obtained from the Experimental Animal Center of the Xi'an Jiaotong University and housed in a temperature controlled environment (24.0 ± 2.0 °C) with a 12 h light-dark cycle and free ad libitum access to food and water.

2.3. Experimental protocol

C57BL/6J mice are a well-established animal model of diet-induced obesity [23]. Mice were acclimatized to the new environment for two

weeks before experiments and then randomly divided into the following groups ($n = 8$), i.e., 1). The LFD group where mice were fed with low fat diet with 10% kcal originating from fat; 2). The LFD + PYR group, mice of which fed with low fat diet and treated with PYR (3 mg/kg/d) by intragastric (i.g.) for 22 weeks; 3). The HFD group, mice of which fed with HFD containing 45% kcal of fat; 4). The HFD + PYR group, mice of which fed with HFD and treated with PYR (3 mg/kg/d) i.g. for 22 weeks. At the end of experiments (mice at age of 28 weeks), the mice were sacrificed and analyzed (The experimental protocol is shown in Fig. 1A).

2.4. Cell line and culture

The HUVEC line was purchased from the American Type Culture Collection (#CRL-1730; ATCC, Manassas, VA, USA). Cells were grown in Ham's F12K medium (Macgene Biotech Co., Ltd., Beijing, China) supplemented with 0.03 mg/ml endothelial cell growth supplement (Macgene Biotech Co., Ltd), 10% fetal bovine serum (FBS; Hyclone, Logan, UT, USA) and 1× Penicillin-Streptomycin Solution (Beyotime Biotech, Haimen, China) in a humidified incubator with 95% air and 5% CO_2 at 37 °C. Cells between passage 3 and 6 were used for the experiments.

2.5. Cell treatment

HUVECs were treated with 30 mM D-glucose for 0, 12, 24, 48, 72 h to investigate the effects of hyperglycemia on HUVEs ER stress and O-GlcNAc level. Glucosamine (GlcN, 7.5 mM) was also used to mimic the effects of chronic hyperglycemia in part of the experiment. Except when investigating the effects of ACh on ER stress and O-GlcNAcylation, HUVEs were incubated with D-glucose (30 mM, 48 h) in the presence of 10^{-8} M, 10^{-7} M, 10^{-6} M, 10^{-5} M ACh. Controls were performed in the presence of media with normal D-glucose (Con, 5 mM).

Cells were randomly divided into the following groups for further treatment: 1) Con: cultured with normal glucose (5 mM) for 48 h; 2) ACh: treatment with ACh (10^{-6} M) alone for 48 h; 3) HG: incubated with high glucose (HG, 30 mM) for 48 h; 4) HG + ACh: cells were treated with ACh (10^{-6} M) for 30 min, and then cultured in high glucose (30 mM) for 48 h; 5) GlcN: treated with glucosamine (7.5 mM) for 48 h; 6) GlcN + ACh: after ACh (10^{-6} M) treatment for 30 min, cells were then cultured in glucosamine (7.5 mM) for 48 h; 7) HG + ACh + 4-DAMP: cells were treated with 4-DAMP (a selective M3 AChR antagonist, 10^{-6} M) for 30 min and cultured as the same as in HG + ACh group for 48 h; 8) HG + ACh + Comp C: Treated with Comp C (the AMPK inhibitor, 10^{-8} M) for 30 min and cultured as the same as in HG + ACh group for 48 h; 9) AICAR: after AICAR (the AMPK activator, 10^{-6} M) incubation cells were exposed to glucose (30 mM) treatment for 48 h; 10) 4-PBA: after 4-PBA (the ER stress inhibitor, 10^{-4} M) incubation, cells were exposed to glucose (30 mM) treatment for 48 h; 11) DON: after DON (the GFAT antagonists, 5×10^{-8} M) incubation, cells were exposed to glucose (30 mM) treatment 48 h.

2.6. Western blot

Thoracic arterial tissues were homogenized and HUVECs were harvested and incubated in the ice-cold RIPA lysis buffer (Beyotime Biotech, Haimen, China) containing 1 mM phenylmethylsulfonyl fluoride and then centrifuged to collect the supernatants and stored at −80 °C. Protein samples (30 μg) were separated in sodium dodecyl sulfonate (SDS)-polyacrylamide gel electrophoresis gels and transferred to polyvinylidene difluoride membranes (PVDF; Millipore, Billerica, MA, USA). The membranes were blocked with 5% non-fat milk for 1 h at room temperature and then incubated with primary antibodies [i.e., anti-O-GlcNAc (1:800; Sigma-Aldrich), anti-GFAT1 (1:1000; Abcam, Cambridge, MA, USA), anti-OGT (1:1000; Sigma-Aldrich), anti-OGA (1:1000; Bioworld Technology Inc., Louis Park, MN, USA), anti-XBP-1 (1:800; Abcam), anti-BIP (1:1000, Cell Signaling Technology, Beverly, MA, USA), anti-CHOP (1:500, Abbkine, CA, USA), anti-AMPK (1:800, Cell Signaling Technology), anti-pAMPK (1:800, Cell Signaling Technology), and anti-GAPDH (1:5000; CMCTAG, Milwaukee, WI, USA)] at 4 °C overnight. The membranes were washed on the next day with Tris-based saline-Tween 20 (TBS-T) and then incubated with the secondary antibody (1:5000; Cowin Biotech, Beijing, China) for 40 min at room temperature. After washing, the protein bands were visualized using the ECL-Plus reagent (Millipore) and GAPDH was used as a loading control. The blots were quantified using a Gel-Pro Analyzer (Media Cybernetics, Bethesda, MD, USA).

2.7. Hematoxylin and eosin staining and immunohistochemistry

Mice thoracic aorta specimens were isolated and fixed in 4% paraformaldehyde in phosphate-buffered saline (PBS) for 24 h, dehydrated, embedded in paraffin, and sectioned to 5-μm tissue slides using the Leica RM-2135 microtome (Leica, Bensheim, Germany). The tissue sections were used for hematoxylin and eosin (H&E) staining or immunohistochemistry (IHC). The antibodies used for IHC were the O-GlcNAcylation markers: anti-O-GlcNAc (1:100; clone CTD 110.6), anti-GFAT (1:100; Abcam), anti-OGT (1:100; Sigma-Aldrich), and anti-OGA (1:100; Bioworld Technology, Inc.). IHC was performed according to a previous study (15). The sections were washed in PBS and incubated with the streptavidin-biotin-enzyme complex (SABC) kit (Bosterbio, Wuhan, China) and 3, 3′-diaminobenzidine (DAB) peroxidase substrate kit (Bioss, Beijing, China) according to the manufacturer's instructions. The immunostained tissue sections were observed, scored, and photographed under a light microscopy (Olympus BX51, Tokyo, Japan).

2.8. TUNEL (terminal deoxynucleotidyl (TdT) transferase dUTP-biotin nick end-labeling) assay

To assess HUVEC apoptosis, following the different treatments cells were labeled with the DeadEnd Fluorometric TUNEL system (Promega, Madison, WI, USA) according to the manufacturer's protocol. Briefly, HUVECs were cultured and treated in laser confocal petri dishes and then fixed in 4% paraformaldehyde, labeled with TUNEL reaction reagents, and stained with 4′,6-diamidino-2-phenylindole (DAPI) for visualization of cell nuclei. HUVECs were observed under an inverted fluorescence microscope (TE-2000U, Nikon, Japan) for at least 10 randomly selected fields with 400 DAPI-positive cells. The number of TUNEL-positive cells was summarized as percentage (%) of positive nuclei/total nuclei x 100% according to a previous study [24].

2.9. Statistical analysis

Data were presented as mean ± standard error of mean (SEM). Differences between the groups were analyzed with one-way or two-way analysis of variance (ANOVA), followed by Tukey's post hoc test for multiple comparisons using GraphPad Prism 7.0 (GraphPad Software, La Jolla, CA, USA). Results were considered significant when $P < 0.05$.

3. Results

3.1. PYR protection of high fat diet-induced body weight and blood glucose levels

In this study, we established a mouse model of HFD-induced obesity. Animal body weight and blood glucose levels were all significantly increased after 22 weeks of HFD feeding, and PYR treatment dramatically decreased bodyweight ($P < 0.001$) (Fig. 1B) and blood glucose levels ($P < 0.01$) (Fig. 1C). For animals fed a control low fat diet (LFD) there was no significant difference in bodyweight and blood glucose levels with PYR treatment($P > 0.05$) (Fig. 1B&C).

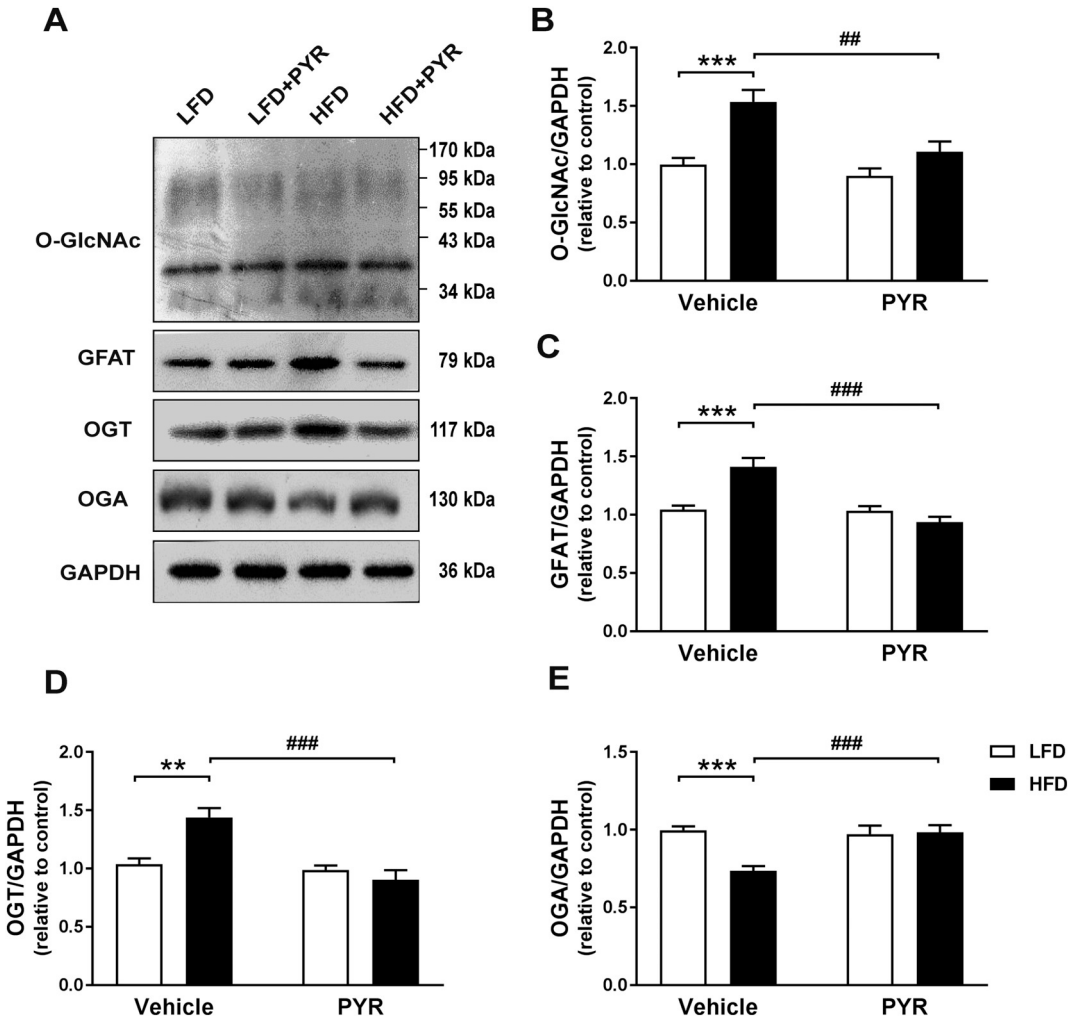

Fig. 2. Effects of HFD and PYR treatment on O-GlcNAcylation in mice thoracic aorta. A: Representative Western blots of O-GlcNAc, GFAT, OGT, OGA and GAPDH. B–E: Quantitative analysis results of the expression of O-GlcNAc, GFAT, OGT, OGA. Results are presented as mean ± SEM ($n = 8$). The effect of HFD was detected by two-way ANOVA for O-GlcNAc ($P < 0.01$), GFAT ($P < 0.001$), OGT ($P < 0.001$) and OGA ($P < 0.05$), while PYR affected O-GlcNAc ($P < 0.001$), GFAT ($P < 0.05$), OGT ($P < 0.05$) and OGA ($P < 0.01$) protein levels. Interaction between HFD and PYR affected O-GlcNAc ($P < 0.05$), GFAT ($P < 0.001$), OGT ($P < 0.01$) and OGA ($P < 0.01$) protein levels as detected by two-way ANOVA. Significant between-group differences from post hoc Tukey test are given as follows: $^{**}P < 0.01$ vs. LFD: Vehicle, $^{***}P < 0.001$ vs. LFD: Vehicle; $^{\#\#}P < 0.01$ vs. HFD: Vehicle, $^{\#\#\#}P < 0.001$ vs. HFD: Vehicle.

3.2. PYR regulation of expression of O-GlcNAc-related proteins in thoracic aorta

To investigate changes in O-GlcNAcylation, we assessed expression of O-GlcNAc-modified proteins, GFAT, OGT, and OGA by Western blot in thoracic arterial tissues. HFD-fed mice exhibited an increase in O-GlcNAc-modified proteins relative to LFD controls that was mitigated with PYR treatment ($P < 0.01$) (Fig. 2B). Moreover, level of GFAT and OGT expression, O-GlcNAc modification enzymes, was significantly upregulated in vascular tissues of the HFD group. Similarly, PYR treatment significantly attenuated the increase in expression following HFD feeding ($P < 0.001$) (Fig. 2C&D). In addition, expression of OGA, a hydrolytic enzyme that removes O-GlcNAc moieties, was significantly lower in the HFD group than that in the LFD group ($P < 0.001$). PYR treatment significantly reversed the HFD-induced reduction of OGA expression in thoracic arterial tissues ($P < 0.001$) (Fig. 2E).

3.3. PYR protection of HFD-induced O-GlcNAc and structure damage in thoracic aorta

We assessed expression of O-GlcNAc-modified proteins, GFAT, OGT and OGA in thoracic arterial tissues using immunohistochemistry. Similar to our western blot results, we observed a qualitative increase in O-GlcNAcylation levels in thoracic arteries of obese mice after 22 weeks of HFD that was as apparent with PYR treatment (Fig. 3A). Moreover, expression of GFAT and OGT was significantly enhanced in the HFD group relative to the LFD group. However, PYR treatment attenuated the increase in GFAT and OGT caused by HFD (Fig. 3BC). Interestingly, OGA was visually decreased in the thoracic arteries of obese mice, but was restored with PYR treatment (Fig. 3D).

Histologically, the smooth muscle layers in the HFD group were directly exposed to the vessel lumen because of endothelial cell desquamation compared with that of the LFD group, (Fig. 3E). However, as shown in Fig. 3E, PYR treatment reduced HFD-induced changes in endothelium structural morphology.

3.4. ACh decreased O-GlcNAcylation via M3 AChR/AMPK/ER stress pathway in HUVECs

O-GlcNAcylation was first monitored in HUVECs after exposure to HG for 0, 12, 24, 48, and 72 h. HG culture of HUVECs resulted in higher O-GlcNAc levels compared to the control group, and significant differences were apparent at 48 h ($P < 0.05$) (Fig. 4A). This result demonstrates that hyperglycemia treatment induced a time-dependent

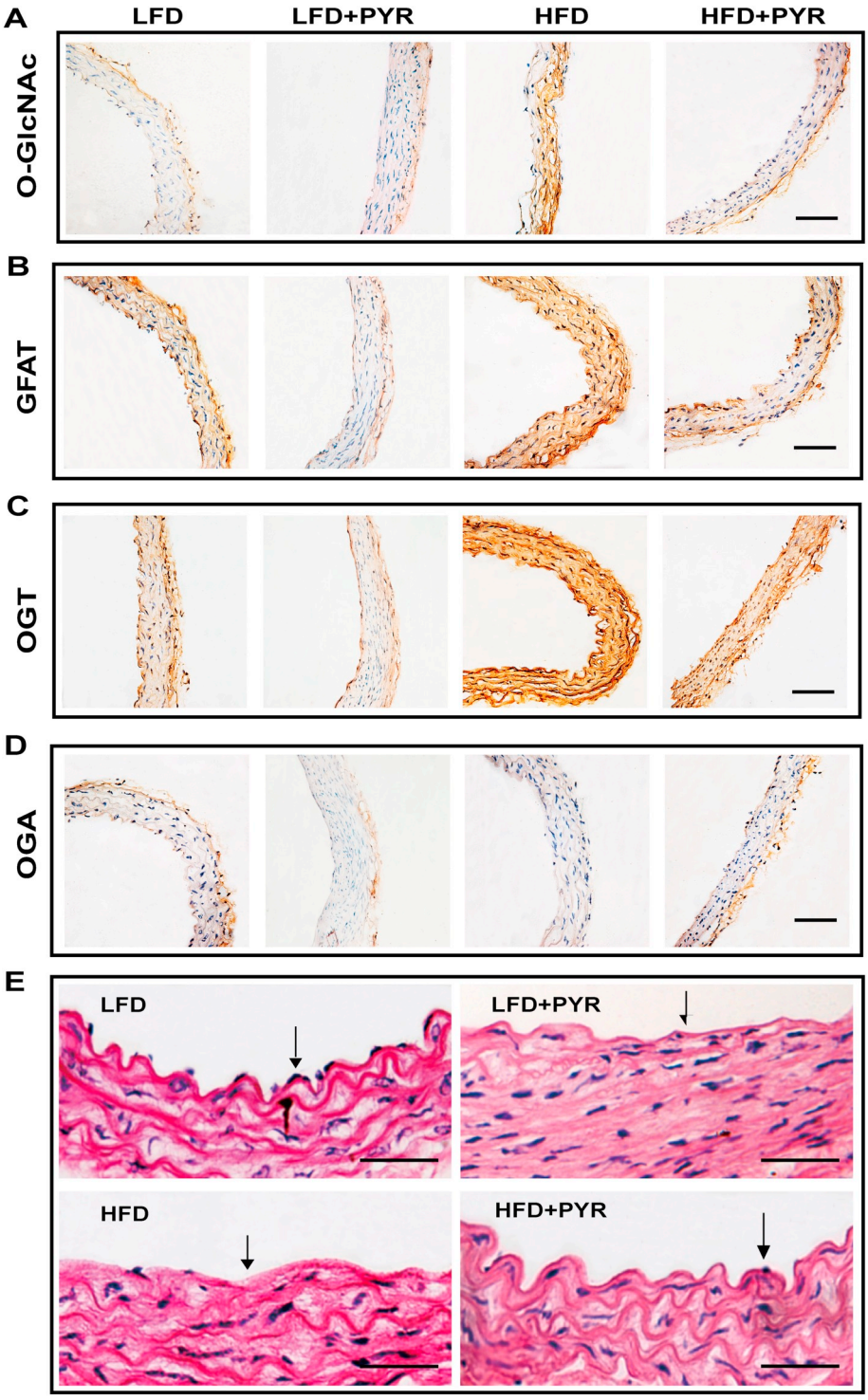

Fig. 3. Effects of PYR treatment on HFD-induced progression of O-GlcNAc on IHC staining and structure damage in thoracic aorta. A–D: Representative images of O-GlcNAc, GFAT, OGT and OGA stained with IHC (400 × magnification). Positive immunoreaction is observed as brown precipitate. Blue color represents the nucleus in cells. Scale bar = 50 μm. E: H&E stained images. Scale bar = 50 μm. Blue color represents the nucleus and red represents the cytoplasm. Arrows indicate endothelial cells. (For interpretation of the references to colour in this figure legend, the reader is referred to the web version of this article.)

rise of O-GlcNAc levels in HUVECs. HFD-induced increases in O-GlcNAc levels were ameliorated after ACh treatment (10^{-8}–10^{-5} M) in a dose-dependent manner ($P < 0.01$, $P < 0.001$) (Fig. 4B). Following these experiments, we used ACh at a concentration of 10^{-6} M.

To investigate changes in O-GlcNAcylation in HG-induced HUVECs, we assessed level of O-GlcNAc-modified proteins, GFAT, OGT, and OGA using Western blot. We found that HG induced O-GlcNAcylation and expression of O-GlcNAc, GFAT, and OGT ($P < 0.01$, $P < 0.001$, $P < 0.05$). ACh treatment attenuated HG-induced O-GlcNAcylation and expression of O-GlcNAc, GFAT, and OGT ($P < 0.01$, $P < 0.001$, $P < 0.05$) (Fig. 4D-G). Similar to our *in vivo* observations, expression of OGA was significantly lower in HG group than in the control group ($P < 0.01$) and ACh treatment significantly reversed HG induced reduction of OGA expression ($P < 0.01$; Fig. 4F).

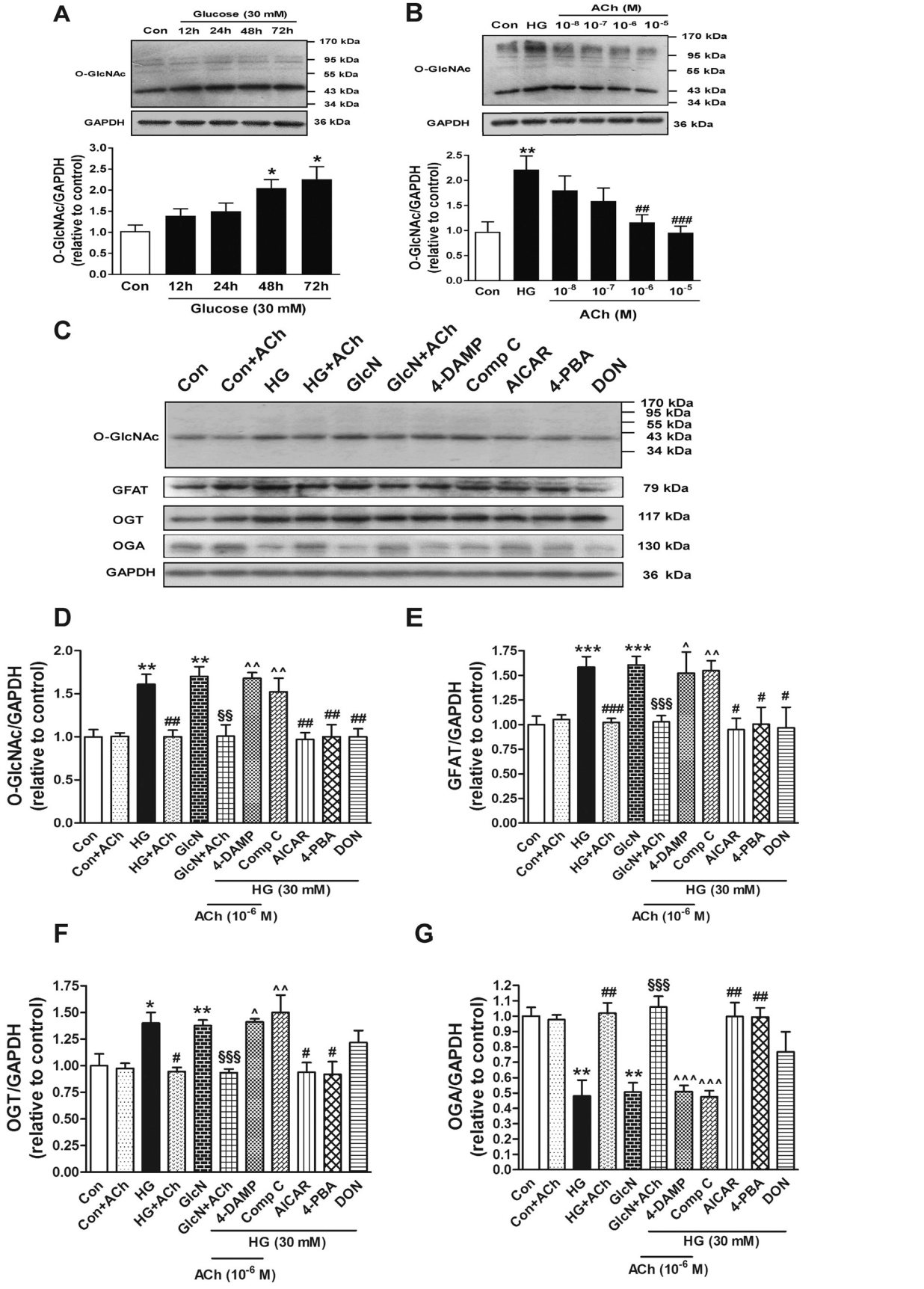

(caption on next page)

Fig. 4. ACh decreased the O-GlcNAcylation via M3 AChR/AMPK/ER stress pathway in HUVECs. To further clarify the potential mechanism of the ACh-mediated protective effect, 4-DAMP (a selective M3AChR antagonist, 10^{-6} mol/L), Comp C (an AMPK inhibitor, 10^{-8} mol/L) were used in combination with ACh (10^{-6} mol/L) and HG (30 mM). AICAR (an AMPK activator, 10^{-6} mol/L), 4-PBA (an ER stress inhibitor, 10^{-4} mol/L), DON (a GFAT antagonists, 5×10^{-8} mol/L) were used in combination with HG (30 mM). A: Treatment of HUVECs with HG for indicated time intervals, representative immunoblots and quantitative analysis of O-GlcNAc. B: ACh diminished HG-induced O-GlcNAc levels in a dose-dependent manner. C: Representative immunoblots for O-GlcNAc, GFAT, OGT and OGA. D-G: Quantitative analysis results of the expression of O-GlcNAc, GFAT, OGT and OGA. Results are presented as mean ± SEM ($n = 4$). For statistical analysis, one-way ANOVA followed by Tukey post hoc test was used. $^{*}P < 0.05$ vs. Con, $^{**}P < 0.01$ vs. Con, $^{***}P < 0.001$ vs. Con; $^{\#}P < 0.05$ vs. HG, $^{\#\#}P < 0.01$ vs. HG, $^{\#\#\#}P < 0.001$ vs. HG; $^{\S\S}P < 0.01$ vs. GlcN, $^{\S\S\S}P < 0.001$ vs. GlcN; $^{\wedge}P < 0.05$ vs. HG + ACh, $^{\wedge\wedge}P < 0.01$ vs. HG + ACh, $^{\wedge\wedge\wedge}P < 0.001$ vs. HG + ACh.

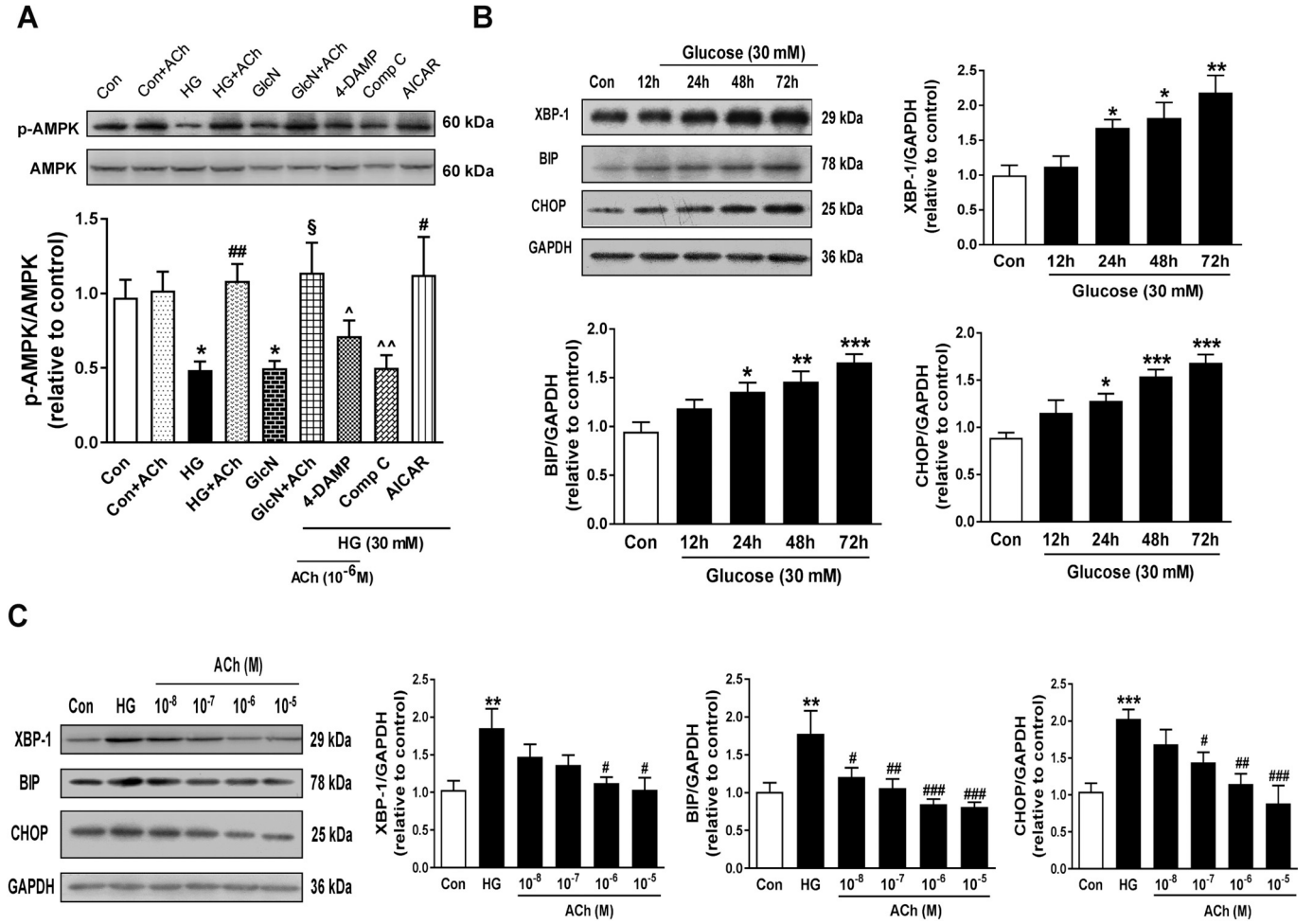

Fig. 5. ACh-mediated AMPK signaling and in a dose-dependent manner attenuated HG-induced ER stress. To further clarify the potential mechanism of the ACh-mediated protective effect, 4-DAMP (a selective M3AChR antagonist, 10^{-6} mol/L), Comp C (the AMPK inhibitor, 10^{-8} mol/L) were used in combination with ACh (10^{-6} mol/L) and HG (30 mM). AICAR (the AMPK activator, 10^{-6} mol/L) was used in combination with HG (30 mM). A: ACh increased the phosphorylation of AMPK after HG, which was blocked by 4-DAMP and Comp C. B: Treatment of HUVECs with HG for indicated time intervals, representative immunoblots and quantitative analysis of XBP-1, BIP and CHOP. C: ACh diminished HG-induced ER stress in endothelial cells in a dose-dependent manner. Results are presented as mean ± SEM ($n = 4$). A value of $P < 0.05$ was considered statistically significant. For statistical analysis, one-way ANOVA followed by Tukey post hoc test was used. $^{*}P < 0.05$ vs. Con, $^{**}P < 0.01$ vs. Con, $^{***}P < 0.001$ vs. Con; $^{\#}P < 0.05$ vs. HG, $^{\#\#}P < 0.01$ vs. HG, $^{\#\#\#}P < 0.001$ vs. HG.

To dissect the role of signaling components of ACh's actions to reduced HG-induced changes in O-GlcNAcylation, we used a number of well-described pharmacological tools. 4-DAMP (an M3 AChR inhibitor, 10^{-6} M), Comp C (a nonselective inhibitor of AMPK, 10^{-8} M), AICAR (an AMPK activator, 10^{-6} M), 4-PBA (an ER stress inhibitor, 10^{-4} M), and DON (a GFAT antagonist, 5×10^{-8} M) were used in the present study. The effect of ACh on HG-induced O-GlcNAcylation was abolished by 4-DAMP and Comp C, while AICAR, 4-PBA, and DON showed the similar effect of ACh. These data demonstrate an important role of M3 AChR/AMPK in ACh-elicited inhibition of HG-induced O-GlcNAcylation in HUVECs. Furthermore, 4-PBA also reduced levels of O-GlcNAcylation compared with HG group, indicating that inhibition of ER stress could decrease O-GlcNAcylation levels. The results suggest that during HG-induced endothelial cell apoptosis, ER stress activation might precede O-GlcNAcylation induction.

3.5. ACh-mediated AMPK signaling dose-dependently attenuates hyperglycaemia-induced ER stress

AMPK activation protects endothelial cells from hypoxia/reoxygenation (H/R)-induced injury by inhibition of ER stress and apoptosis. Therefore, we evaluated the role of AMPK activation in the context of ACh in HG-induced endothelial cells injury. As shown in Fig. 5A, HG and GlcN reduced phosphorylated AMPK levels compared to the control group ($P < 0.05$), whereas ACh treatment restored phosphorylated AMPK in the presence of HG ($P < 0.01$). This effect was

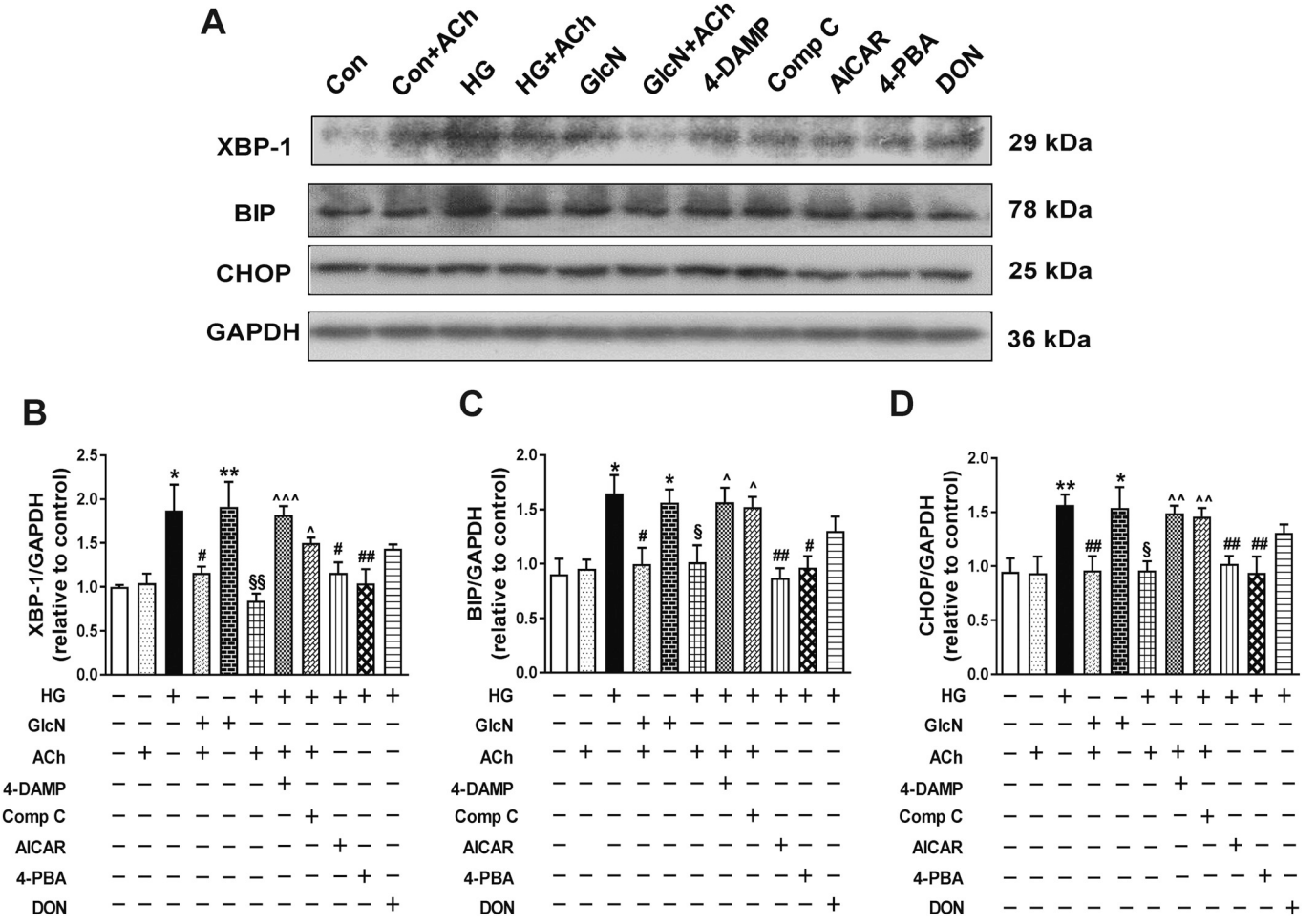

Fig. 6. ACh inhibited ER stress via M3 AChR/AMPK. To further clarify the potential mechanism of the ACh-mediated protective effect, 4-DAMP (a selective M3AChR antagonist, 10^{-6} mol/L), Comp C (an AMPK inhibitor, 10^{-8} mol/L) were used in combination with ACh (10^{-6} mol/L) and HG (30 mM). AICAR (the AMPK activator, 10^{-6} mol/L), 4-PBA (an ER stress inhibitor, 10^{-4} mol/L), DON (a GFAT antagonists, 5×10^{-8} mol/L) were used in combination with HG (30 mM). A: Representative immunoblots for XBP-1, BIP and CHOP. B-D: Quantitative analysis results of the expression of XBP-1, BIP and CHOP. Results are presented as mean ± SEM ($n = 4$). For statistical analysis, one-way ANOVA followed by Tukey post hoc test was used. $^{*}P < 0.05$ vs. Con, $^{**}P < 0.01$ vs. Con; $^{\#}P < 0.05$ vs. HG, $^{\#\#}P < 0.01$ vs. HG; $^{\S}P < 0.05$ vs. GlcN, $^{\S\S}P < 0.01$ vs. GlcN; $^{\wedge}P < 0.05$ vs. HG + ACh, $^{\wedge\wedge\wedge}P < 0.001$ vs. HG + ACh.

abolished by 4-DAMP and Comp C ($P < 0.05$, $P < 0.01$). AICAR showed the similar effect of ACh ($P < 0.05$). These results suggest that AMPK may play an important role in ACh-induced endothelial protection in HUVECs *in vitro*.

HUVECs were then exposed to HG for 0, 12, 24, 48, or 72 h, after which we assessed ER stress biomarkers, like XBP-1, BIP, and CHOP. As shown in Fig. 5B, expression of XBP-1, BIP, and CHOP was significantly increased in response to HG stimulation for 24 h compared with those of the control group ($P < 0.05$). We found that ACh reduced expression levels of ER stress markers triggered by HG in cells. HG-induced expression of XBP-1, BIP and CHOP was attenuated by ACh pre-treatment (10^{-8}–10^{-5} M) in a dose-dependent manner, indicating that ACh was able to inhibit HG-induced ER stress in HUVECs. Based on these results, ACh was used at the concentration of 10^{-6} M in the remaining experiments.

3.6. ACh inhibition of the ER stress by activation M3 AChR

As shown in Fig. 6, HG treatment enhanced ER stress, evident by an increase in the level of ER stress markers XBP-1, BIP, and CHOP ($P < 0.05$, $P < 0.01$). On the contrary, ACh treatment significantly reduced such an increase in XBP-1, BIP and CHOP expression ($P < 0.05$, $P < 0.01$) (Fig. 6B–D), which was further confirmed by cotreatment with 4-DAMP, Comp C, AICAR, 4-PBA, and DON. The protective effect of ACh was blocked by treatment of 4-DAMP and Comp C, while AICAR and 4-PBA treatment showed similar effects with ACh, which further confirmed the role of ACh in HUVEC protection from HG and indicates that the M3 AChR/AMPK plays a role in ACh alleviated HG-induced ER stress in HUVECs. Interestingly, DON treatment significantly reduced O-GlcNAcylation levels ($P < 0.01$), but did not affect ER stress levels ($P > 0.05$). These data are consistent with the hypothesis that ER stress might occur prior to O-GlcNAcylation under HG conditions.

3.7. ACh inhibition of HG-induced apoptosis in HUVECs

Caspase-3 activation was assessed by Western blot and cell apoptosis was measured using the TUNEL assay. As shown in Fig. 7, cleaved caspase-3 and the number of TUNEL-positive cells was significantly increased in the HG group ($P < 0.001$, $P < 0.05$), whereas ACh treatment significantly attenuated the HG-induced TUNEL-positive cells and cleaved caspase-3 ($P < 0.001$, $P < 0.05$) (Fig. 7). Treatment with 4-DAMP and Comp C mitigated the anti-apoptotic effect of ACh ($P < 0.05$), suggesting that M3 AChR/AMPK plays an essential role in ACh-induced endothelial protection from HG-induced injury.

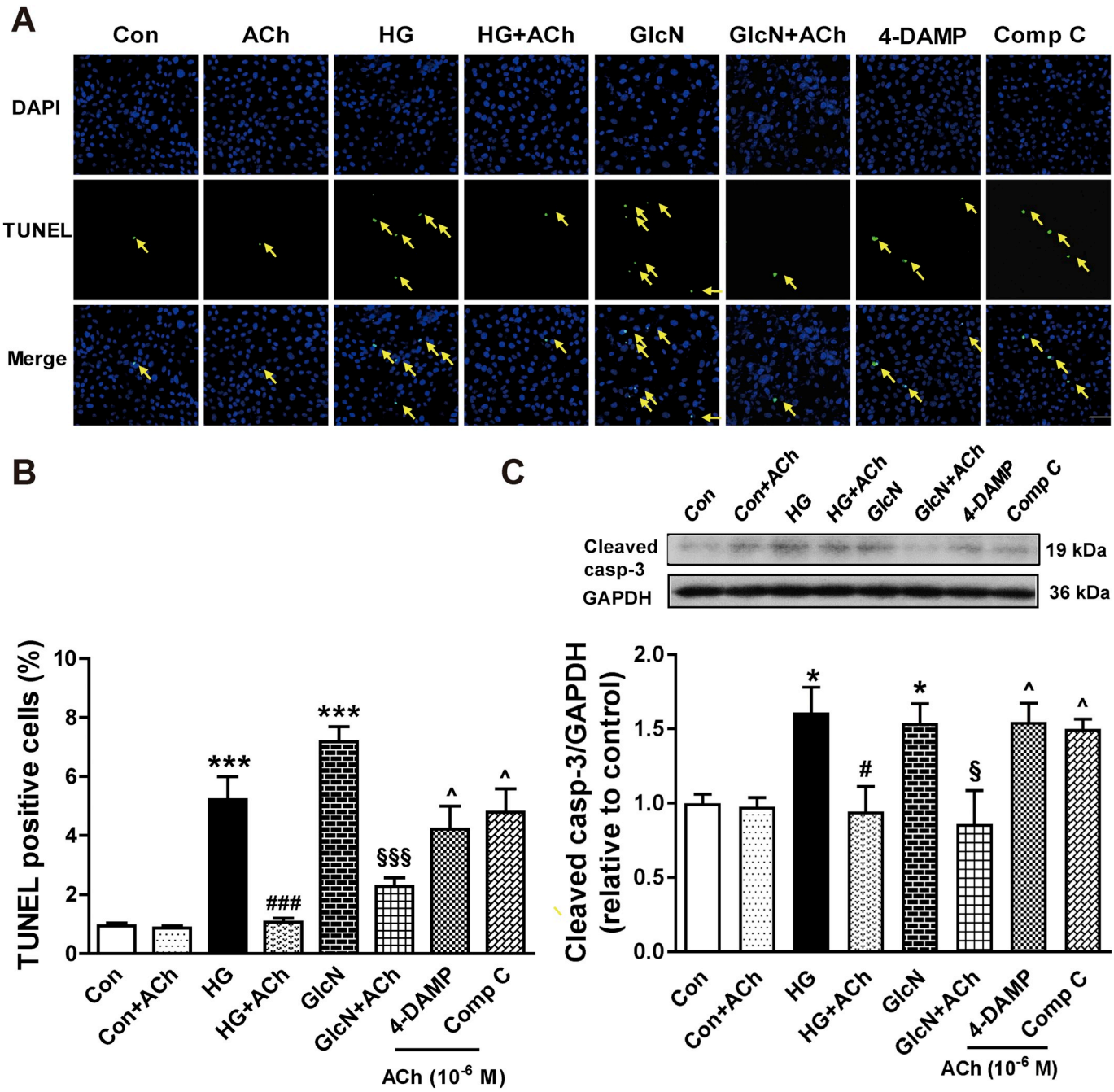

Fig. 7. ACh inhibits HG-induced cell apoptosis. To further clarify the potential mechanism of the ACh-mediated protective effect, 4-DAMP (a selective M3AChR antagonist, 10^{-6} mol/L), Comp C (an AMPK inhibitor, 10^{-8} mol/L) were used in combination with ACh (10^{-6} mol/L) and HG (30 mM). A and B: TUNEL assay measured cells death in different groups. Scale bar = 50 um. C: The changes of cleaved caspase-3 expression were examined by Western blot. Results are presented as mean ± SEM ($n = 4$). For statistical analysis, one-way ANOVA followed by Tukey post hoc test was used.*$P < 0.05$ vs. Con, ***$P < 0.001$ vs. Con; $^{\#}P < 0.05$ vs. HG, $^{\#\#\#}P < 0.001$ vs. HG; $^{\S}P < 0.05$ vs. GlcN, $^{\S\S\S}P < 0.001$ vs. GlcN; $^{\wedge}P < 0.05$ vs. HG + ACh.

4. Discussion

Obesity induces both structural and functional damage in the vasculature, which may be associated with metabolic disorders of lipid and glucose [25]. However, the underlying molecular mechanisms linking hyperglycemia to vascular injury are undefined in the context of obesity. Increased level of O-GlcNAc and ER stress activation are important contributors to endothelial cell dysfunction. Nonetheless, the effect of hyperglycemia on O-GlcNAcylation, the ER stress, and vascular dysfunction needs further investigation. The main findings of the study shown in Fig. 8. HFD led to an increase in body weight and blood glucose, augmented O-GlcNAc levels, and produced structural damage in thoracic aorta endothelium. In cultured cells, elevated glucose was associated with the activation of ER stress upon hyperglycemia promoted the O-GlcNAcylation accumulation, and these changes ultimately resulted in endothelial cells apoptosis. PYR significantly decreased body weight and blood glucose, and reduced the level of O-GlcNAc, as well as qualitatively improved vessel structural damage in mouse thoracic aortal tissues. ACh suppressed HG-induced ER stress activation, O-GlcNAc level accumulation, and cell apoptosis. *In vitro* analyses demonstrated that HG triggered ER stress activation, elevated O-GlcNAc levels, and induced subsequent apoptosis in endothelial cells.

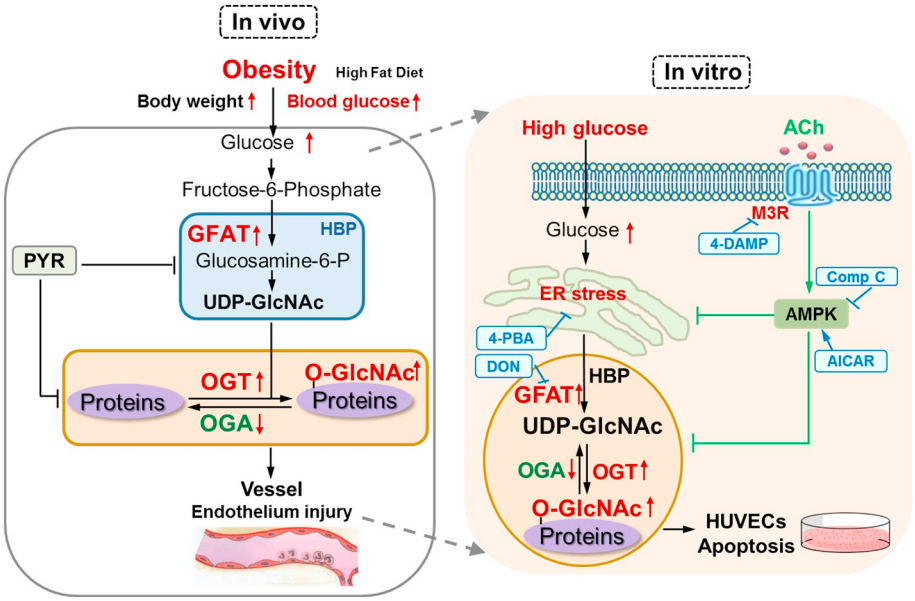

Fig. 8. The putative mechanism underlying PYR-induced vascular protection of thoracic aorta. PYR: pyridostigmine; HBP: hexosamine biosynthetic pathway; GFAT: glutamine fructose-6-phosphate amidotransferase; UDP-GlcNAc: UDP-*N*-acetyl-glucosamine; O-GlcNAc: O-linked β-*N*-acetylglucosamine; OGT: O-GlcNAc transferase; OGA: β-*N*-acetylglucosaminidase; IHC: immunohistochemistry; ACh, acetylcholine; AMPK, AMP-activated protein kinase; CHOP, C/EBP homologous protein; ER, endoplasmic reticulum; M3 AChR, type-3 muscarinic acetylcholine receptor; TUNEL, terminal deoxynucleotidyl transferase mediated dUTP-biotin nick end labeling; 4-DAMP, 4-diphenylacetoxy-*N*-methylpiperidine methiodide; 4-PBA, 4-phenyl butyric acid; DON, *O*-diazoacetyl-L-serine (azaserine) and 6-diazo-5-oxonorleucine; Comp C, Compound C; AICAR, 5-aminoimidazole-4-carboxamide ribose; BIP, binding immunoglobulin protein; XBP1, X box-binding protein. i.g.: intragastric administration.

The M3 AChR-AMPK signaling pathway plays a pivotal role in protection effect of ACh on HUVECs upon HG. Collectively, these findings indicate that O-GlcNAcylation may represent an additional mechanism that underlies vascular dysfunction in obesity and that PYR-induced restoration of thoracic aorta endothelium structural damage in obese mice is possibly associated with a decrease in O-GlcNAc levels, and that ER stress may play a crucial role in the regulation O-GlcNAc levels. The M3 AChR-AMPK pathway was also responsible for ACh-afforded endothelial protection.

C57BL/6J mice have been widely used as an important model of diet-induced diabetes, obesity and metabolic syndrome [26,27]. However, C57BL/6J mice naturally lack nicotinamide nucleotide transhydrogenase (*Nnt*) protein, which is linked to glucose intolerance and reduced insulin secretion [28,29]. A recent study from our laboratory showed that serum glucose levels were elevated in HFD-fed C57BL/6J mice and that PYR treatment significantly decreased serum glucose levels in mice of the HFD + PYR group (30). In our current study, PYR reduced blood glucose levels in the HFD + PYR group, which is consistent with a previous study [30]. Recent evidence indicates that increased O-GlcNAcylated proteins were involved in cardiovascular diseases, diabetes, and obesity [31–34]. It is well established that augmented O-GlcNAcylation enhanced vascular reactivity to vasoconstrictive stimuli and impaired nitric oxide (NO)-dependent arteriolar dilations [35–37]. In the current study, H&E staining revealed that due to degradation of endothelial structure in HFD-fed mice aorta, the smooth muscle layers were directly exposed to the vessel lumen. There was also a difference in O-GlcNAcylation level between the thoracic aorta tissues of the LFD and HFD group. Levels of O-GlcNAcylation, GFAT, and OGT were significantly increased, but OGA expression was significantly reduced in HFD-fed mice. These results suggest that O-GlcNAc could play a role in obesity-induced vascular injury, which is consistent with the previous data reported by Lima et al. who showed that O-GlcNAcylation in the vasculature of hypertensive rats impaired endothelium-dependent relaxation and enhanced sensitivity to vasoconstrictors [38,39]. Of importance, treatment with PYR reversed these changes. PYR significantly reduced the level of O-GlcNAcylation, decreased GFAT and OGT expression, and increased OGA expression to improve the vascular endothelium structure. These results indicate that PYR-decreased O-GlcNAc and the alleviation in vascular endothelium damage may be through inhibition of GFAT over-expression and restoration of OGT and OGA balance in the blood vessels. Taken together, these results suggest that HFD-induced vascular damage may occur in the vessel endothelium and the protective effect of PYR treatment may be due to the prevention of HFD-induced increases in O-GlcNAc.

PYR, a reversible cholinesterase inhibitor increases serum ACh levels by decreasing AChE activity [20]. Therefore, HUVECs were administrated by HG and/or ACh in order to investigate the mechanisms of PYR on O-GlcNAcylation. *In vitro* experiments demonstrated that HG triggered O-GlcNAc elevated levels by increasing the expression of GFAT and OGT, decreasing OGA level, and inducing subsequent apoptosis in endothelial cells. HUVECs were exposed to HG for varying durations (0, 12, 24, 48, 72 h) to assess ER stress and O-GlcNAcylation. HG enhanced ER stress and O-GlcNAcylation levels, and ER stress activation occurred upstream of the increase in O-GlcNAcylation levels. Further, ACh suppressed HG-induced ER stress activation, O-GlcNAc level accumulation, and cell apoptosis. These results indicate that PYR may play a directly role in the reduction of O-GlcNAcylation level, suggesting that ER stress is possibly involved in the process of O-GlcNAcylation augment induced by HG.

A growing number of studies have speculated that HBP was connected with the ER stress responses. HBP was recently shown to be activated by ER stress through the Xbp1-dependent transcription of GFAT, a rate-limiting enzyme of HBP [40]. While glucosamine treatment increased flux through HBP induction of ER stress activation [13]. In this study, HUVECs were treated with HG and GlcN, mimic the effect of chronic hyperglycemia, to investigate that the link between activation of ER stress response and total cellular O-GlcNAcylation level in hyperglycemia treatment endothelial cells. Incubation of HUVECs with HG and GlcN not only enhanced the ER stress and O-GlcNAcylation level, but also showed that ER stress activation occurred upstream of the increase in O-GlcNAcylation. Moreover, the level of ER stress markers expression was not affected following inhibition of O-GlcNAcylation by using DON, the GFAT antagonist. The O-GlcNAcylation level was restored when HUVECs exposed to HG and incubated with 4-PBA, the ER-stress inhibitor. Collectively, these data provide evidence for the coupling of ER stress and HBP under HG conditions in culture.

In addition, we assessed the possible mechanism of attenuating ER stress, O-GlcNAcylation and apoptosis in HUVECs using ACh. Previous studies have demonstrated that ACh prevents endothelial cells apoptosis induced by multiple pathological insults, including H/R or I/R, likely through M3 AChR [41–43]. Consistent with those results, in this study, ACh was able to activate M3 ACh receptors to reduce ER stress, O-GlcNAcylation, and expression of apoptosis markers, while the M3 AChR inhibitor 4-DAMP was able to abolish the effects of ACh that

restore the levels of ER stress, O-GlcNAcylation, and apoptosis in HG-cultured HUVECs. It was observed that HG negatively affected p-AMPK expression, whereas ACh treatment resulted in a restoration of p-AMPK activity, indicating the role of ACh in modulation of the AMPK pathway. Furthermore, activation or blockage of p-AMPK activity using its activator AICAR or inhibitor Comp C, respectively showed that AICAR decreased ER stress, O-GlcNAcylation, and apoptosis, whereas Comp C could increase ER stress and O-GlcNAcylation level to promote cell apoptosis. Indeed, previous studies from our lab showed that ACh treatment benefited the heart and endothelium through activation of M3 AChR [42,43]. Both M3 AChR siRNA and 4-DAMP abolished the protective effect of ACh on cells and M3 AChR siRNA blocked the ACh-induced restoration of AMPK activity under H/R [22]. These results suggested that the M3 AChR-AMPK pathway play a role in the beneficial effects of ACh.

However, our current study does have some limitations; for example, our *in vitro* data showed that the AMPK inhibitor Compound C was able to abolish the protective effect of ACh on ER-stress, but our current data do not provide a direct support of the ER stress downstream of AMPK. Thus, it is unclear what the exact signals induced by HG to regulate the ER-stress are. Thus, a future study needs to define these signals.

5. Conclusion

In conclusion, the current study demonstrates that PYR was able to protect vascular endothelium damage induced by HFD by decreasing the level of O-GlcNAcylation. ACh ameliorated HG-induced apoptosis of HUVECs by regulation of the M3 AChR/AMPK to reduce the ER stress and O-GlcNAcylation. The data from the current study indicate that O-GlcNAcylation in blood vessels could represent an additional mechanism underlying vascular dysfunction in obesity and provide a novel insight into a better understanding of cholinergic drugs PYR and ACh induced vascular protection effects.

Conflict of interest

The authors declare that there are no conflicts of interest.

Acknowledgement

This work was supported by grants from National Natural Science Foundation of China (No. 81770293, No. 81473203, and No. 81872868).

References

[1] X.D. Chao, Y.H. Ma, P. Luo, L. Cao, W.B. Lau, B.C. Zhao, et al., Up-regulation of heme oxygenase-1 attenuates brain damage after cerebral ischemia via simultaneous inhibition of superoxide production and preservation of NO bioavailability, Exp. Neurol. 239 (2013) 163–169.
[2] A.M. Beyer, D.F. Guo, K. Rahmouni, Prolonged treatment with angiotensin 1-7 improves endothelial function in diet-induced obesity, J. Hypertens. 31 (2013) 730–738.
[3] Y. Zhang, J. Ren, Epigenetics and obesity cardiomyopathy: from pathophysiology to prevention and management, Pharmacol. Ther. 161 (2016) 52–66.
[4] S. Wang, C. Wang, S. Turdi, et al., ALDH2 protects against high fat diet-induced obesity cardiomyopathy and defective autophagy: role of CaM kinase II, histone H3K9 methyltransferase SUV39H, Sirt1, and PGC-1α deacetylation, Int. J. Obes. 42 (5) (2018) 1073–1087.
[5] E. Selvin, S. Marinopoulos, G. Berkenblit, T. Rami, F.L. Brancati, N.R. Powe, S.H. Golden, Meta-analysis: glycosylated hemoglobin and cardiovascular disease in diabetes mellitus, Ann. Intern. Med. 141 (2004) 421–431.
[6] M. Kozakova, C. Palombo, C. Morizzo, K. Hojlund, M. Hatunic, B. Balkau, et al., Obesity and carotid artery remodeling, Nutr. Diabetes 5 (2015) e177.
[7] T.V. Fiorentino, A. Prioletta, P. Zuo, F. Folli, Hyperglycemia-induced oxidative stress and its role in diabetes mellitus related cardiovascular diseases, Curr. Pharm. Des. 19 (2013) 5695–5703.
[8] J.A. Hanover, M.W. Krause, D.C. Love, The hexosamine signaling pathway: O-GlcNAc cycling in feast or famine, Biochim. Biophys. Acta 1800 (2) (2010) 80–95.
[9] N.E. Zachara, N. O'Donnell, W.D. Cheung, J.J. Mercer, J.D. Marth, G.W. Hart, Dynamic O-GlcNAc modification of nucleocytoplasmic proteins in response to stress. A survival response of mammalian cells, J. Biol. Chem. 279 (29) (2004) 30133–30142.
[10] V.V. Lima, F.R. Giachini, T. Matsumoto, W. Li, A.F. Bressan, D. Chawla, et al., High-fat diet increases O-GlcNAc levels in cerebral arteries: a link to vascular dysfunction associated with hyperlipidaemia/obesity? Clin. Sci. (Lond.) 130 (2016) 871–880.
[11] S. Lenna, R. Han, M. Trojanowska, Endoplasmic reticulum stress and endothelial dysfunction, Int. Union Biochem. Mol. Biol. 66 (8) (2014) 530–537.
[12] S. Wang, X. Chen, S. Nair, et al., Deletion of protein tyrosine phosphatase 1B obliterates endoplasmic reticulum stress-induced myocardial dysfunction through regulation of autophagy, Biochim. Biophys. Acta Mol. basis Dis. 1863 (12) (2017) 3060–3074.
[13] W. Qiu, R. Kohen-Avramoglu, S. Mhapsekar, J. Tsai, R.C. Austin, K. Adeli, Glucosamine-induced endoplasmic reticulum stress promotes ApoB100 degradation: evidence for Grp78-mediated targeting to proteasomal degradation, Arterioscler. Thromb. Vasc. Biol. 25 (3) (2005) 571–577.
[14] G.A. Ngoh, T. Hamid, S.D. Prabhu, S.P. Jones, O-GlcNAc signaling attenuates ER stress-induced cardiomyocyte death, Am. J. Physiol. Heart Circ. Physiol. 297 (5) (2009) H1711–H1719.
[15] J.C. Chatham, L.G. Nöt, N. Fülöp, R.B. Marchase, Hexosamine biosynthesis and protein O-glycosylation: the first line of defense against stress, ischemia, and trauma, Shock 29 (4) (2008) 431–440.
[16] G.A. Ngoh, L.J. Watson, H.T. Facundo, W. Dillmann, S.P. Jones, Non-canonical glyco-syltransferase modulates post-hypoxic cardiac myocyte death and mitochondrial permeability transition, J. Mol. Cell. Cardiol. 45 (2) (2008) 313–325.
[17] L.J. Chaar, Coelho A1, N.M. Silva, W.L. Festuccia, V.R. Antunes, High-fat diet-induced hypertension and autonomic imbalance are associated with an upregulation of CART in the dorsomedial hypothalamus of mice, Physiol. Rep. 4 (11) (2016), https://doi.org/10.14814/phy2.12811 (pii: e12811).
[18] K. Lim, B. Barzel, S.L. Burke, J.A. Armitage, G.A. Head, Origin of aberrant blood pressure and sympathetic regulation in diet-induced obesity, Hypertension. 68 (2) (2016) 491–500.
[19] S. Banni, G. Carta, E. Murru, L. Cordeddu, E. Giordano, F. Marrosu, M. Puligheddu, G. Floris, G.P. Asuni, A.L. Cappai, S. Deriu, P. Follesa, Vagus nerve stimulation reduces body weight and fat mass in rats, PLoS One 7 (9) (2012) e44813.
[20] Y. Lu, Q. Wu, L.Z. Liu, X.J. Yu, J.J. Liu, M.X. Li, W.J. Zang, Pyridostigmine protects against cardiomyopathy associated with adipose tissue browning and improvement of vagal activity in high-fat diet rats, BBA-Mol. Basis Dis. 1864 (2018) 1037–1050.
[21] F. Qin, Y. Lu, X. He, M. Zhao, X. Bi, X. Yu, et al., Pyridostigmine prevents peripheral vascular endothelial dysfunction in rats with myocardial infarction, Clin. Exp. Pharmacol. Physiol. 41 (2014) 202–209.
[22] X.Y. Bi, X. He, M. Xu, M. Zhao, X.J. Yu, X.Z. Lu, W.J. Zang, Acetylcholine ameliorates endoplasmic reticulum stress in endothelial cells after hypoxia/reoxygenation via M3 AChR-AMPK signaling, Cell Cycle 14 (2015) 2461–2472.
[23] K. Rooney, S.E. Ozanne, Maternal over-nutrition and offspring obesity predisposition: targets for preventative interventions, Int. J. Obes. 35 (2011) 883–890.
[24] L. Yu, Q. Li, B. Yu, Y. Yang, Z. Jin, W. Duan, G. Zhao, M. Zhai, L. Liu, D. Yi, M. Chen, S. Yu, Berberine attenuates myocardial ischemia/reperfusion injury by reducing oxidative stress and inflammation response: role of silent information regulator 1, Oxidative Med. Cell. Longev. 2016 (2016) 1689602.
[25] J.J. Reho, K. Rahmouni, Oxidative and inflammatory signals in obesity-associated vascular abnormalities, Clin. Sci. (Lond.) 131 (2017) 1689–1700.
[26] K. Kaku, F.T. Fiedorek Jr., M. Province, et al., Genetic analysis of glucose tolerance in inbred mouse strains: evidence for polygenic control, Diabetes 37 (1988) 707–713.
[27] S. Kooptiwut, S. Zraika, A.W. Thorburn, et al., Comparison of insulin secretory function in two mouse models with different susceptibility to beta-cell failure, Endocrinology 143 (2002) 2085–2092.
[28] T.T. Huang, M. Naeemuddin, S. Elchuri, et al., Genetic modifiers of the phenotype of mice deficient in mitochondrial superoxide dismutase, Hum. Mol. Genet. 15 (2006) 1187–1194.
[29] H.C. Freeman, A. Hugill, N.T. Dear, et al., Deletion of nicotinamide nucleotide transhydrogenase a new quantitive trait locus accounting for glucose intolerance in C57BL/6J mice, Diabetes 55 (2006) 2153–2156.
[30] R.Q. Xue, X.J. Yu, M. Zhao, et al., Pyridostigmine alleviates cardiac dysfunction via improving mitochondrial cristae shape in a mouse model of metabolic syndrome, Free Radic. Biol. Med. 134 (2019) 119–132.
[31] S.Y. Li, Y. Liu, V.K. Sigmon, A. McCort, J. Ren, High-fat diet enhances visceral advanced glycation end products, nuclear O-Glc-Nac modification, p38 mitogen-activated protein kinase activation and apoptosis, Diabetes Obes. Metab. 7 (2005) 448–454.
[32] B. Laczy, B.G. Hill, K. Wang, A.J. Paterson, C.R. White, D. Xing, Y.F. Chen, V. Darley-Usmar, S. Oparil, J.C. Chatham, Protein O-GlcNAcylation: a new signaling paradigm for the cardiovascular system, Am. J. Physiol. Heart Circ. Physiol. 296 (2009) H13–H28.
[33] W.B. Dias, G.W. Hart, O-GlcNAc modification in diabetes and Alzheimer's disease, Mol. BioSyst. 3 (2007) 766–772.
[34] N. Fulop, R.B. Marchase, J.C. Chatham, Role of protein O-linked N-acetyl-glucosamine in mediating cell function and survival in the cardiovascular system, Cardiovasc. Res. 73 (2007) 288–297.
[35] V.V. Lima, F.R. Giachini, F.S. Carneiro, Z.N. Carneiro, Z.B. Fortes, M.H.C. Carvalho, R.C. Webb, R.C. Tostes, Increased vascular O-GlcNAcylation augments reactivity to constrictor stimuli, JASH, 2 2008, pp. 410–417.
[36] V.V. Lima, F.R. Giachini, H. Choi, F.S. Carneiro, Z.N. Carneiro, Z.B. Fortes, M.H. Carvalho, R.C. Webb, R.C. Tostes, Impaired vasodilator activity in deoxycorticosterone acetate-salt hypertension is associated with increased protein O-

GlcNAcylation, Hypertension 53 (2009) 166–174.
[37] V.V. Lima, F.R. Giachini, F.S. Carneiro, Z.N. Carneiro, M.A. Saleh, D.M. Pollock, Z.B. Fortes, M.H. Carvalho, A. Ergul, R.C. Webb, et al., O-GlcNAcylation contributes to augmented vascular reactivity induced by endothelin 1, Hypertension 55 (2010) 180–188.
[38] Z.V. Wang, Y. Deng, N. Gao, Z. Pedrozo, D.L. Li, C.R. Morales, A. Criollo, X. Luo, W. Tan, N. Jiang, M.A. Lehrman, B.A. Rothermel, A.H. Lee, S. Lavandero, P.P.A. Mammen, A. Ferdous, T.G. Gillette, P.E. Scherer, J.A. Hill, Spliced X-box binding protein 1 couples the unfolded protein response to hexosamine biosynthetic pathway, Cell 156 (6) (2014) 1179–1192.
[39] X. He, X.Y. Bi, X.Z. Lu, M. Zhao, X.J. Yu, L. Sun, M. Xu, W.G. Wier, W.J. Zang, Reduction of mitochondria-endoplasmic reticulum interactions by acetylcholine protects human umbilical vein endothelial cells from hypoxia/reoxygenation injury, Arterioscler. Thromb. Vasc. Biol. 35 (7) (2015) 1623–1634.
[40] M. Xu, X.Y. Bi, X. He, X.J. Yu, M. Zhao, W.J. Zang, Inhibition of the mitochondrial unfolded protein response by acetylcholine alleviated hypoxia/reoxygenation-induced apoptosis of endothelial cells, Cell Cycle 15 (2016) 1331–1343.
[41] M. Zhao, X. He, X.Y. Bi, X.J. Yu, W. Gil Wier, W.J. Zang, Vagal stimulation triggers peripheral vascular protection through the cholinergic anti-inflammatory pathway in a rat model of myocardial ischemia/reperfusion, Basic Res. Cardiol. 108 (2013) 345.
[42] Y. Miao, X.Y. Bi, M. Zhao, H.K. Jiang, J.J. Liu, D.L. Li, X.J. Yu, Y.H. Yang, N. Huang, W.J. Zang, Acetylcholine inhibits tumor necrosis factor a activated endoplasmic reticulum apoptotic pathway via EGFR-PI3K signaling in cardiomyocytes, J. Cell. Physiol. 230 (2015) 767–774.
[43] L. Sun, W.J. Zang, H. Wang, M. Zhao, X.J. Yu, X. He, Y. Miao, J. Zhou, Acetylcholine promotes ROS detoxification against hypoxia/reoxygenation-induced oxidative stress through FoxO3a/PGC-1a dependent superoxide dismutase, Cell. Physiol. Biochem. 34 (2014) 1614–1625.